

# Experimental Study on the Viscoelastic Behaviors of Debris Flow Slurry

WANG Yuyi<sup>1,2\*</sup>, TAN Rongzhi<sup>1,2</sup>, HU Kaiheng<sup>1,2</sup>, CHEN Feiyue<sup>3</sup>, YANG Hongjuan<sup>1,2</sup>, ZHANG Jinshan<sup>1,2</sup>, LV Juan<sup>2</sup>

*1 Key Laboratory of Mountain Hazards and Earth Surface Process, Dongchuan Debris Flow Observation and Research Station, Chinese Academy of Sciences, Chengdu 610041, China*

*2 Institute of Mountain Hazards and Environment, Chinese Academy of Sciences, Chengdu 610041, China*

*3 Shanghai Representative Office, Anton Paar GmbH, Shanghai 200040, China*

\*Corresponding author, e-mail: wyyzou@imde.ac.cn

© Science Press and Institute of Mountain Hazards and Environment, CAS and Springer-Verlag Berlin Heidelberg 2012

**Abstract:** The rheological properties of most liquid in nature are between liquids and solids, including both elastic changes and viscosity changes, that is so-called “viscoelastic”. Dynamic oscillatory test was used to quantitatively study the distinct viscoelastic behaviors of debris flow slurry in the shear stress conditions for the first time in this study. The debris flow slurry samples were from Jiangjiagou Ravine, Yunnan Province, China. The experimental results were found that at the low and middle stages of shearing, when the angular velocity  $\omega < 72.46 \text{ s}^{-1}$ , the loss modulus ( $G''$ ) was greater than the storage modulus ( $G'$ ), i.e.  $G'' > G'$ . At the late stage of shearing, when the angular velocity  $\omega \geq 72.46 \text{ s}^{-1}$ , the storage modulus was greater than or equal to the loss modulus, i.e.  $G' \geq G''$ ,  $\tan \delta \leq 1$  (where phase-shift angle  $\delta = G''/G'$ ), and the debris flow slurry was in a gel state. Therefore, the progress of this experimental study further reveals the mechanism of hyperconcentrated debris flows with a high velocity on low-gradient ravines.

**Keywords:** Loss modulus ( $G''$ ); Storage modulus ( $G'$ ); Viscoelastic behaviors; Gel state

## Introduction

The rheological properties of most liquid in nature are between liquids and solids, including both elastic changes and viscosity changes, that is so-called “viscoelastic”. Viscoelasticity is the property of materials that exhibit both viscous and elastic characteristics when undergoing deformation. Viscous materials resist shear flow and strain linearly with time when a stress is applied. Elastic materials strain instantaneously when stretched and just as quickly return to their original state once the stress is removed. Viscoelastic materials have elements of both of these properties and, as such, exhibit time dependent strain. Viscoelastic materials can be modeled in order to determine their stress or strain interactions as well as their temporal dependencies. These models, which include the Maxwell model, the Kelvin-Voigt model, and the Standard Linear Solid Model, are used to predict a material's response under different loading conditions. Viscoelastic behavior has elastic and viscous components modeled as linear combinations of springs and dashpots, respectively (Huang et al.

**Received:** 28 December 2011

**Accepted:** 8 May 2012

1983). While debris flow slurry has distinct viscoelastic behaviors in the shear stress conditions.

The rheological properties of viscous debris flow are the basis for studying the motion mechanism of debris flow. The previous studies mainly focused on the observation experiments of the rheological model of viscous debris flow and determining its parameters (Bagnold 1994; Jan et al. 1997; Schatzmann et al. 2003; Shen et al. 1998; Wang et al. 2000; Wang et al. 2004). The rippling creep phenomena of viscous debris flow on deposit fan and the bedding structure of accumulation patterns were also noted, and the initial understanding that hyperconcentrated debris flow had the viscoelastic behaviors displayed by the Weissenberg effect was made (Major 1994; Wang et al. 2009). But the quantitative test and analysis about the viscoelastic behaviors of different viscous debris flows from triggering, thixotropy and shearing movement were not developed both at home and abroad for the restrictions of rheological equipments.

The rheological dynamic oscillatory tests were made to study the debris flow slurry from Jiangjiagou Ravine with the further rheological research at home and abroad, especially the recent use of new strain oscillatory rheometer. These tests quantitatively explored the viscoelastic properties of slurry samples, including the characteristics of storage modulus ( $G'$ ), loss modulus ( $G''$ ) and complex modulus ( $G^*$ ) with the changing of angular velocity (frequency), and the correlation between them. The experimental results were found: at the low and middle stages of shearing, when the angular velocity  $\omega < 72.46 \text{ s}^{-1}$ , the loss modulus was greater than the storage modulus, i.e.  $G'' > G'$ ; when  $\omega \cong 2.15 \text{ s}^{-1}$ , the complex modulus ( $G^*$ ) showed the behavior of shear thinning; when  $\omega \cong 3.16 \text{ s}^{-1}$ , the complex modulus increased with the increasing of angular velocity. The increasing rate was the power law index of 1.041. At the late stage of shearing, when the angular velocity  $\omega \cong 72.46 \text{ s}^{-1}$ , the storage modulus was greater than or equal to the loss modulus, i.e.  $G' \cong G''$ ,  $\tan \delta \cong 1$  (where phase-shift angle  $\delta = G''/G'$ ), and the debris flow slurry was in a gel state. These findings and analysis bring new progress to the study on rheological behaviors of debris flow, further reveal rheological behavior of slope loose mass from solid to liquid and also explain that the

hyperconcentrated viscous debris flow is like cement concrete which is just made, and is like solid mass with viscous, elastic and plastic behaviors. Therefore, this experiment further explains why hyperconcentrated viscous debris flow (with the volume concentration of solid up to 80%) can rapidly move on low-gradient ( $3^\circ$ - $5^\circ$ ) ravines with velocity in the range of 10-18  $\text{m}\cdot\text{s}^{-1}$ .

## 1 Experimental Method

Viscoelastic behavior has elastic and viscous components modeled as linear combinations of springs and dashpots, respectively. In an equivalent electrical circuit, stress is represented by voltage and the derivative of strain (velocity) by current. The elastic modulus of a spring is analogous to a circuit's capacitance (it stores energy) and the viscosity of a dashpot to a circuit's resistance (it dissipates energy). Within the elastic limit, the ratio of stress ( $\tau$ ) and strain ( $e$ ) is called storage modulus; when over the elastic limit, the ratio of stress ( $\tau$ ) and strain ( $e$ ) is called loss modulus. Many fluids show distinctive viscoelastic properties under shear stress conditions.

The increasingly popular test method is to give an oscillatory stress to viscoelastic sample instead of a constant stress which generates steady flow. The time-related strain values are measured by applying a constant shear rate or a constant shear stress for each single measuring point (Equation (1)) (Gebhard 1998). The oscillation experiment method by rheometer is to put the sample in the shear gap and give a certain strain, so there will be impedance stress in the sample. Then the relationship between oscillatory stress and strain can be obtained. So the oscillatory stress test is often referred as "dynamic test". This method is to find the relationship between set angular velocity (or frequency) and the resulting oscillating stress or strain, and to provide the viscoelastic data related to time response.

$$\tau = \tau_0 * \sin(\omega * t) \quad (1)$$

The forced oscillatory tests of debris flow slurry were made with MCR-301 rheometer produced by Anton Paar. The rotary flat plate system of this instrument was used, and the interval between the two plates was 3 mm. The

samples were fine-grained soil of debris flows at Jiangjiagou Ravine, with the particle size distribution as shown in Figure 1,  $d_{max}=1$  mm, and the content of clay ( $< -8 \phi$ ) was 38.6%. The density of prepared debris flow slurry was  $1.622 \text{ g}\cdot\text{cm}^{-3}$  and the solid volume concentration was 0.3659. The parallel and repeated trials of oscillatory dynamic tests of the same sample were made, just the interval between the two plates was 2.7mm, and the results were consistent with the former results. The angular velocity (frequency,  $\omega \text{ s}^{-1}$ ) of oscillatory test ranged from 0.1 to 100 ( $\text{s}^{-1}$ ), the experimental temperature was  $20^\circ\text{C}$ , and the following viscoelastic parameters of debris flow slurry were measured: loss modulus  $G''$ , storage modulus  $G'$  and complex viscosity  $\eta^*$ , in which  $\eta^*$  was different from the viscosity general measured in shear, but it is the oscillatory tests result.

All the experimental method and data collection are made according to the instruction book of MCR-301 rheometer produced by Anton Paar.

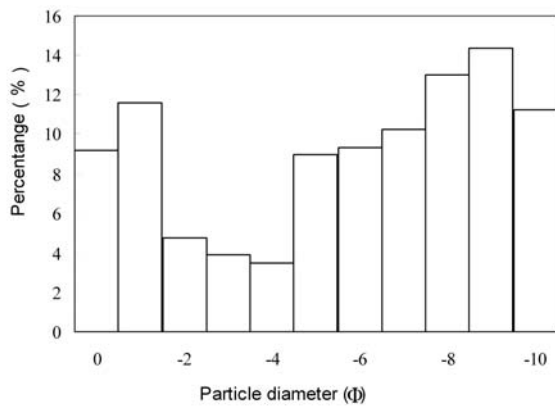


Figure 1 Particle composition ( $\phi$ ) in debris flow

## 2 Results and Analysis

The analysis of viscoelastic behaviors of debris flow slurry was made through using the method of Gauss coordinate system (Gebhard 1998) and Pythagoras's law (Haake information report 1991) and combining with the characteristics of debris-flow deformation and motion.

### 2.1 Gauss coordinate system showing $G'$ , $G''$ , $\eta^*$ and $\omega$

The method of Gauss coordinate system

(Gebhard 1998) can be used to distinct the viscous and elastic behaviors of the sample during dynamic tests. In the Gauss coordinate system with real axis and imaginary axis, the complex can be expressed in vector form. Therefore complex modulus  $G^*$  can be defined as Equation (2) in Gauss coordinate system, when notation of  $G'$  and  $G''$  as sine and cosine functions (Equation (3) and Equation (4)),  $\tau_0, \gamma_0$  as the maximum of stress and strain respectively, and  $\delta$  as the phase-shift angle of the response to stress and strain.

In Equation (2) (Gebhard 1998), storage modulus  $G'$  expresses the stress energy stored temporarily and can be regained later, while loss modulus  $G''$  is irreversible loss of deformation energy which has changed into shearing heat.

$$G^* = G' + i G'' = \tau_0(t) / \gamma_E(t) \tag{2}$$

$$G' = (\tau_0 / \gamma_0) \cos \delta \tag{3}$$

$$G'' = (\tau_0 / \gamma_0) \sin \delta \tag{4}$$

Ideal viscous behavior can be specified in terms of  $\delta=90^\circ, G'=0$  or as  $G''=G^*$ . Ideal elastic behavior can be expressed as  $\delta=0^\circ, G'=G^*$  or as  $G''=0$ .

Therefore complex viscosity  $\eta^*$  can be defined as Equation (5) to express the total resistance forces of the sample in dynamic shearing instead of  $G^*$  (Gebhard 1998).

$$\eta^* = G^* / \omega = \tau_0 / \gamma_0 \cdot \omega \tag{5}$$

The viscoelastic behavior expressed by hyperbolas in Figure 2 is similar to that of collagen (Gebhard 1998; Thomas et al. 2006). The hyperbolas in Figure 2 show the elastic response and viscous flow in certain degree when sinusoidal

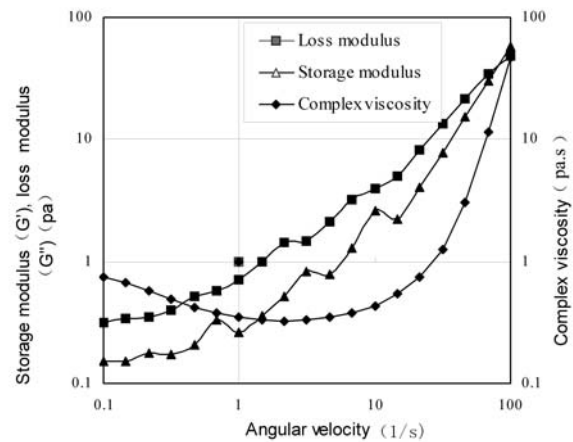


Figure 2 The relationship between loss modulus, storage modulus and angular velocity of debris flow slurry

stress is given to debris flow slurry. When the angular velocity is  $0.1 \text{ s}^{-1}$ , loss modulus is  $1.29 \text{ Pa}$  greater than storage modulus.

With the increasing of angular velocity, the curve of  $\log G''$  increases with the slope of  $\tan \alpha=0.742$ , while the curve of  $\log G'$  increases with the slope of  $\tan \alpha=0.834$ . When the angular velocity is  $68.1 \text{ s}^{-1}$ , the values of  $G'$  and  $G''$  are similar. Therefore, the increasing rate of elastic response is greater than that of viscous response at high shearing rate. When  $\omega=100 \text{ s}^{-1}$  or higher, the elastic response is greater than viscous response. At low angular velocity ( $\omega < 2.15 \text{ s}^{-1}$ ), complex viscosity  $\eta^*$  shows the behavior of shear-thinning. When  $\omega = 2.15 \text{ s}^{-1}$ , complex viscosity becomes the smallest, i.e., the resistance force is the minimum. After that point, complex viscosity quickly increases at the rate of  $\tan \alpha > 1$  with the increasing of angular velocity ( $3.16 \text{ s}^{-1} \leq \omega \leq 100 \text{ s}^{-1}$ ), i.e. the slope of curve  $\log \eta^*$  is  $\tan \alpha = 1.3$ .

This phenomenon is much like the model of viscoelastic combination. According to the dynamic experiment of Maxwell liquid, there are following two cases (Gebhard 1998; Thmas et al. 2006).

$$\text{Case (1): } (\lambda\omega)^2 \ll 1, G' = G(\lambda\omega)^2 \dots G'' = \eta\omega \quad (6)$$

$$\text{Case (2): } (\lambda\omega)^2 \gg 1, G' = G \dots G'' = G^2 / \eta\omega \quad (7)$$

According to the behavior of Maxwell model, in case (1) where the frequency is low, the storage modulus scales as the frequency squared, whereas the loss modulus is proportional to the frequency. In this regime, the viscous component is greater than the elastic component since the model has enough time to respond to a given strain (Gebhard 1998). In case (2) the frequency is high and the dashpot does not have enough time to respond to the given strain. In this regime, the elastic component dominates and the substance behaves like a spring. Therefore, the rheological behaviors of debris flow slurry belong to the typical behaviors of viscoelastic fluid. In a separate study, storage modulus not only increases with the increasing of concentration of debris flow slurry, but also is affected by the content of coarse particles (sand). The higher the proportion of coarse particles is, the greater the storage modulus is.

### 2.2 The theorem of Pythagoras showing the relation of $G'$ , $G''$ , $G^*$ and $\tan \delta$

The viscoelastic behavior of each real material

consists of a viscous and an elastic portion (Haake information report 1991). This sum can be illustrated by a vector diagram when  $G'$  is plotted on the x-axis and  $G''$  on the y-axis (Figure 3), and also can be described by Equation (8). The length of each vector represents the value of the corresponding parameter.  $G^*$  is the vector sum, i.e. the resultant of the two proportions  $G'$  and  $G''$ , therefore characterizing the complete viscoelastic behavior which consists of both the elastic and the viscous portion.

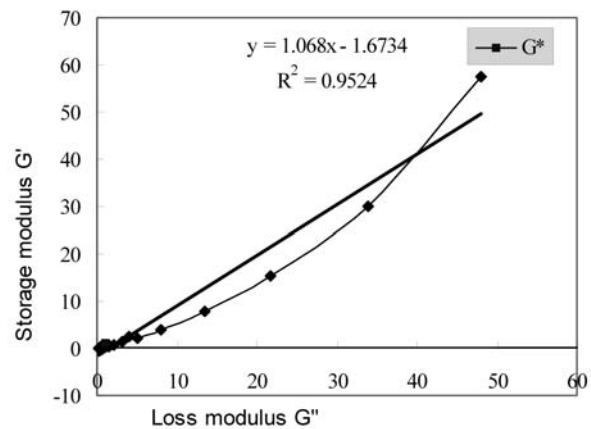


**Figure 3** The vector diagram showing from  $G'$ ,  $G''$  and  $G^*$

The relation between  $G'$ ,  $G''$  and  $G^*$  may be illustrated when using the theorem of *Pythagoras* (philosopher and mathematician in ancient Greek, 570 to 496 BC) concerning the relation between the lengths of the sides of a rectangular triangle (Equation (8)):

$$G^* = \sqrt{(G')^2 + (G'')^2} \quad (8)$$

Based on this trigonometric relation, the loss modulus is illustrated in Figure 2 as the side opposite to  $\delta$  divided by the side adjacent to  $\delta$ , which is defined as the tangent of the angle  $\delta$  (Haake information report 1991):

$$\tan \delta = G'' / G' \quad (9)$$

According to the equation in Figure 3, the slope of  $G^*$  and  $G''$  in this sample is 1.068, i.e., the angle between viscous response and the complex modulus ( $G^*$ ) is  $46.9^\circ (\approx 45^\circ)$ . According to Table 1, it is a very interesting phenomenon, indicating that the coexistence of the viscous response and the elastic response within the changing range of angular velocity, namely when the hyperconcentrated debris flow moves with a high

**Table 1** Rheological behavior from  $\delta$ ,  $\tan \delta$ , loss modulus and storage modulus (Haake Information Report 1991)

Ideal-viscous flow	Viscoelastic liquid	Viscoelastic behavior	Viscoelastic gel or solid	Ideal-elastic deformation
$\delta=90^\circ$	$90^\circ>\delta>45^\circ$	$\delta=45^\circ$	$45^\circ>\delta>0^\circ$	$\delta=0^\circ$
$\tan \delta \rightarrow \infty$	$\tan \delta > 1$	$\tan \delta = 1$	$\tan \delta < 1$	$\tan \delta \rightarrow 0$
$G'' \rightarrow 0$	$G'' > G'$	$G'' = G'$	$G'' < G'$	$G'' \rightarrow 0$

**Note:** Viscoelastic behavior refers to the viscoelastic behavior showing 50/50 of the viscous and elastic portion

speed overall, there are both solid-like behaviors and the behaviors of viscous fluid.

Complex modulus ( $G^*$ ) represents the total resistance forces against the applied strain. The complex modulus and phase-shift angle  $\delta$  of real viscoelastic materials vary with frequency (Haake information report 1991), therefore, frequency sweep should be made within the set range during forced oscillatory tests, the value of  $G^*$  and  $\delta$  with the changing frequency should be measured, then the spectrum line of  $G^*$  and  $\delta$  can be got. The curve of  $\delta$  with the changing frequency increases within the range from  $0^\circ$  to  $90^\circ$ , which indicates that the changes of viscose response and elastic response of the sample in low and high frequency are different. Figure 4 shows the relationship between phase-shift angle and complex modulus of debris flow flurry under angular frequency. At the low frequency of angular velocity ( $0.1\text{-}0.316\text{ s}^{-1}$ ),

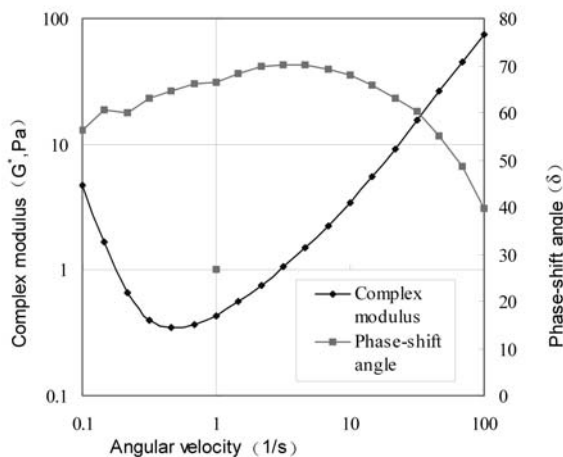


**Figure 4** The relationship between phase-shift angular and complex modulus under angular velocity

complex modulus changes at the rate with the power law index of  $-2.187$  and rapid shears thinning (Equation (10)). When the angular velocity is bigger than  $3.16\text{ s}^{-1}$ , complex modulus increases at the rate with the power-law index of

$1.041$  (Equation (11)), which indicates that the total resistance force of debris flow slurry increases with the increasing of angular velocity (frequency). The changing behaviors of complex modulus are basically consistent with the change of complex viscosity showing in Figure 2.

$$G^* = 0.0275(\omega)^{-2.187} \quad \text{when } \gamma < 0.316\text{s}^{-1} \dots R^2 = 0.9792 \quad (10)$$

$$G^* = 0.416(\omega)^{1.041} \quad \text{when } 0.316\text{s}^{-1} < \gamma < 100\text{s}^{-1} \dots R^2 = 0.9738 \quad (11)$$

The results of debris-flow dynamic oscillatory tests show that the curve of phase-shift angle  $\delta$  changes within the range from  $39.9^\circ$  to  $70^\circ$ . When the angular velocity changes within low frequency range ( $0.1\text{-}3.16\text{ s}^{-1}$ ), phase-shift angle increases at the rate with the power-law index of  $0.061$ , i.e., from  $56.17^\circ$  ( $\omega=0.1\text{ s}^{-1}$ ) to  $70.2^\circ$  ( $\omega=3.16\text{ s}^{-1}$ ). If  $\delta=45^\circ$ , viscoelastic behavior showing 50 to 50 ratio of the viscous and elastic portions, the viscous response gradually increases with the increasing of angular velocity, rising from 62.4% to 78%, while the elastic response decreases relatively (Equation (12)).

However, when  $\omega > 3.16\text{ s}^{-1}$ , the phase-shift angle slightly decreases at the rate with the power-law index of  $0.061$ , i.e., from  $70.11^\circ$  ( $\omega=4.64\text{ s}^{-1}$ ) to  $39.8^\circ$  ( $\omega=100\text{ s}^{-1}$ ). It indicates that the viscous response of the sample gradually reduces, i.e., from 78% to 44%, while the elastic response slightly increases relatively (Equation (13)).

$$\delta = 66.682(\omega)^{0.061} \quad \text{when } \gamma < 3.16\text{s}^{-1} \dots R^2 = 0.9445 \quad (12)$$

$$\delta = 98.656(\omega)^{-0.167} \quad \text{when } 3.16\text{s}^{-1} < \gamma < 100\text{s}^{-1} \dots R^2 = 0.8477 \quad (13)$$

Equation (9) is the ratio of loss modulus to storage modulus, which shows the energy changing characteristics of viscous deformation and elastic

deformation of viscoelastic deformation behaviors. Generally the change of  $\tan \delta$  ranges between 0 and  $\infty$  (Haake information report 1991), showing in equation (14):

$$0 \leq \tan \delta \leq \infty \dots (\sin \text{ce. } 0^0 \leq \delta \leq 90^0) \tag{14}$$

*or. if. in. rad. .0 ≤ δ ≤ π / 2)*

The changing characteristics of  $\delta$ ,  $G'$  and  $G''$  of ideal-viscous and ideal-elastic behaviors have been discussed above, and Table 1 can be further illustrated as follows:

For the liquid state (sol state) holds:

$$\tan \delta > 1 \quad (\text{since } G'' > G')$$

For the gel state (solid state) holds:

$$\tan \delta < 1 \quad (\text{since } G'' < G')$$

At the gel point holds:

$$\tan \delta = 1 \quad (\text{since } G'' = G')$$

### 2.3 The characteristics of the ratio of loss modulus to storage modulus:

The test results and analysis can further confirm that natural gravelly soil (solid) on steep slopes will suddenly become thixotropic liquefaction (liquid) under extreme heavy rainfall.

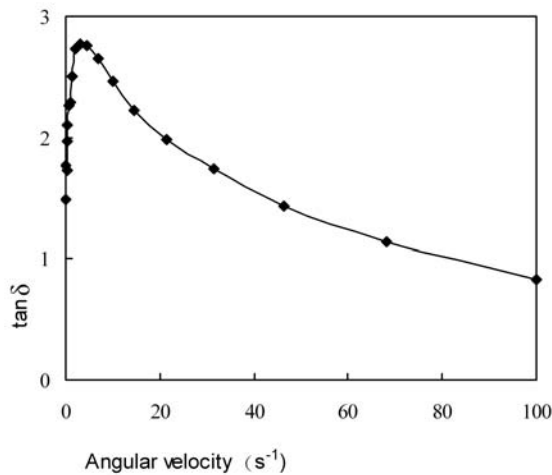


**Figure 5** Changing ratio ( $\tan \delta$ ) of  $G''$  to  $G'$  with angle velocity

Gel state is the critical point.

#### 2.3.1 The change characteristics of $\tan \delta$

Figure 5 shows, with the increasing of angular velocity, there is a turning point of the ratio value ( $\tan \delta$ ) of loss modulus to storage modulus at the

angular velocity of 3.16. At the early stage of low angular velocity ( $\omega \cong 3.16 \text{ s}^{-1}$ ),  $\tan \delta$  increases rapidly at the slope of 0.385 with the increasing of angular velocity (Equation (15)).

When the angular velocity is higher ( $3.16 < \omega \cong 100 \text{ s}^{-1}$ ),  $\tan \delta$  gradually decreases with the increasing of angular velocity, its slope is  $-0.02$  (Equation (16)). The turning point of  $\tan \delta$  is consistent with that of phase-shift angle  $\delta$  showing in Figure 4. While the last two points on the x-axis in Figure 5 show: when  $\omega = 68.1 \text{ s}^{-1}$ ,  $\tan \delta = 1.13 \rightarrow 1$ , i.e.  $\delta = 54.01^\circ$ ; when  $\omega = 100 \text{ s}^{-1}$ ,  $\tan \delta = 0.89 < 1$ , i.e.  $\delta = 39.8^\circ < 45^\circ$ ,  $G'' < G'$ , which indicates debris flow slurry has shown the behavior of viscoelastic gel or solid (Table 1).

$$\tan \delta = 0.385\omega + 1.788 \tag{15}$$

when  $3.16 > \omega > 0.1 \text{ s}^{-1} \dots R^2 = 0.8145$

$$\tan \delta = -0.020\omega + 2.591 \tag{16}$$

when  $100 > \omega > 3.16 \text{ s}^{-1} \dots R^2 = 0.914$

#### 2.3.2 The change characteristics of modulus difference ( $\Delta G$ )

Modulus difference ( $\Delta G$ ) is introduced based on the above analysis to describe the quantitative changes between loss and storage modulus and the turning point from liquid into solid. As shown in Figure 6.

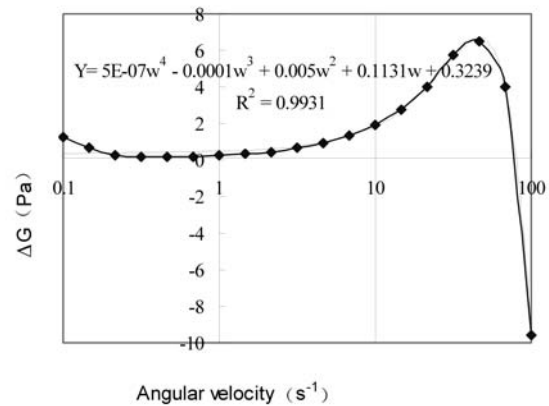


**Figure 6** Modulus difference ( $\Delta G$ ) with angle velocity

If  $\Delta G = G'' - G'$ , then there is fourth order relationship between the modulus difference and angular velocity, and there are four phases of change (Equation (17)).

$$\Delta G = 2e - 06\omega^4 - 0.0003\omega^3 + 0.01\omega^2 + 0.0618\omega + 0.377 \dots R^2 = 0.9904 \tag{17}$$

We discuss the turning point from liquid into solid as following:

(1) The semi-logarithmic curve in Figure 6 shows there are 18 points, whose loss modulus is greater than storage modulus, among the 19 points. At the beginning of deformation ( $\omega_1=0.1 \text{ s}^{-1}$ ), viscous response is 1.29 Pa greater than elastic response (Figure 1), viscous response accounts for 62.4%.

(2) However, when  $0.1 < \omega < 0.464 \text{ s}^{-1}$ ,  $\Delta G$  decreases at the rate with the slope of -1.41 when angular velocity increases, i.e. shear-thinning.  $\Delta G$  decreases from 0.63 Pa ( $\omega_2=0.147 \text{ s}^{-1}$ ) to 0.165 Pa ( $\omega_5=0.464 \text{ s}^{-1}$ ), which shows the increasing rate of viscous response is slightly less than that of elastic response.

(3) When  $0.681 < \omega < 46.4 \text{ s}^{-1}$ , modulus difference ( $\Delta G$ ) significantly increases at the rate with the slope of 1.52 (Equation (18)). During this phase, the increasing rate of viscous response is much higher than that of elastic response, i.e.,  $\Delta G$  increases from 0.189 Pa ( $\omega_6=0.681 \text{ s}^{-1}$ ) to 1.308 Pa ( $\omega_{12} = 6.81 \text{ s}^{-1}$ ) then to 6.5 Pa ( $\omega_{17}=46.4 \text{ s}^{-1}$ ). At this phase, the maximum modulus difference ( $\Delta G, \omega_{17}$ ) is 34.4 times of the minimum modulus difference ( $\Delta G, \omega_6$ ), viscous response increases from 73% to 78%.

(4) When  $46.4 < \omega \leq 100 \text{ s}^{-1}$ , modulus difference ( $\Delta G$ ) indeed decreases at the rate with the slope of -0.31 (Equation 19). If calculated with the Equation (19), when  $\Delta G=0$ , then  $\omega$  is  $72.46 \text{ s}^{-1}$ , i.e.  $G''=G'$ , which indicates the 50 to 50 ratio of viscous response and elastic response. Therefore, this value can be considered as the gel point when debris flow slurry shows behavior of a viscoelastic gel or solid (Table 1).

$$\Delta G = 0.1517\omega + 0.2556 \quad R^2 = 0.9706 \quad (18)$$

$$\Delta G = -0.309\omega + 22.449 \dots R^2 = 9292 \quad (19)$$

### 3 Relationship of Viscoelastic Modulus with Liquefaction and Movement of Debris Flow

For loose soil with many pores in debris flow formation areas (Wang et al. 1999), its mutable modulus is larger than that of the ordinary soil because its permeability and drainage are greater than those of ordinary soil. Therefore, it is difficult

for the slow loading process to cause the excess pore pressure in an actual sense for the soil. However, an abrupt and powerful dynamic loading (for example, earthquakes or strong turbulences) or torrential rain will cause transient excess pore pressure because of the difficulty in the timely dissipation of the interspace water (Vieyamofe 1987; Zhang et al. 1981). Because of the dilating clay particles in the interspace, the drainage in the pore space is reduced. The torrential rain rapidly gets into the pore space. So the water is accumulated on the earth surface and the drainage is slowed down. When there is the excess pore pressure, the soil stress resistance is reduced notably:

$$\tau_s = C + \sigma_s \tan \varphi = C + (\sigma_n - P_e) \tan \varphi \quad (20)$$

Soil stress strength decreases  $P_e \tan \varphi$  because of excess pore pressure. When  $\sigma_n \rightarrow P_e$ , soil stress strength nearly reduces to zero. Therefore it is from this action of the excess pore pressure on the avalanche of debris soil that causes the occurrence of debris flows. So storage modulus < loss modulus at the beginning of debris flow occurrence, and complex viscosity also shows quick shear-thinning. As for the thixotropic rheological property which exists in the debris flow slurry, Wang has studied its sudden, strong destruction, initial phase at a low speed, and the relation between thixotropic energy and thixotropic stress, especially discussed the mechanism of thixotropic initiation and surge flow of viscous debris flow (Wang et al. 2004).

When the volume concentration of hyperconcentrated viscous debris flow is more than 50%, the pore water could not freely transmit the pressure, because the interspaces increase between grains. When the pore outside of the particle is open though, the particle can be acted by water or air pressure. When the pore inside of the particle is closed, in order to support the particle along the vertical direction, it is necessary to increase the excess pressure besides its balance with gravity of the particle in water (Qian 1989). The closer the packing of particles is, the greater excess pressure is. The excess pressure can cause the viscous cohesion between coarse and fine particles, which makes the debris grain suspension. The experiment showed grain weight supported by excess pore pressure is 92.29% of the total weight, i.e., the value of  $P_{gfi}/P_{go}$  is 92.29% (Pierson 1981; Qian

1989; Vieyamofe 1987; Wang et al. 1999; Zhang et al. 1981).

The flocculent structure of debris flow slurry gradually develops a higher density (Zhang et al. 1981), and the higher the density is, the greater the strength of its structure is. The rate of flow speed has played an important role in structural levels in the process of flowing. The structural levels of suspended particles of debris flow will be different in various places of shearing ground in order to adapt to flow speed. The structural levels change with time in various stages. The studies also show that  $P_F$  (the energy value of soil water) will approach zero, when the equivalent pore size  $d_s > 0.3$  mm. When  $d_s = 0.002-0.03$  mm,  $P_F$  is 2-3, the suction of soil water is  $1 \times 10^4 \sim 2 \times 10^5$  Pa. When  $d_s < 0.002$  mm, the suction of soil water is  $2 \times 10^5 \sim 15 \times 10^5$  Pa (or called excess pore pressure) (Yao et al. 1986). Therefore, when the angular frequency is at the middle or high speed in the dynamic oscillatory tests, both loss modulus and storage modulus increase with different degrees.

Iverson (1989) made experiments of dynamic pore pressure fluctuation in rapidly shearing granular materials. He found that the excess pore pressure appears the dynamic balance for texture to be destroyed (pore open) and for texture to resume (pore close). The dynamic oscillation experiments showed that (Figure 5), when the angular velocity was  $100s^{-1}$  in stable shearing movement, the storage modulus of debris flow slurry was 9.5 Pa greater than the loss modulus, i.e.  $\tan \delta < 1$ . The hyperconcentrated viscous debris flow was in a gel state. The following experimental studies combining with the dynamic oscillation experiments of debris flow slurry can further explain that debris flow slurry (its weight ratio is only about 40% of debris flow) of high viscosity ( $\bar{\eta} = 0.177 Pa \cdot s^{-1}$ ) and high yield stress ( $\bar{\tau} = 50.3 Pa$ ) together with coarse particles whose diameter is larger than 2mm (its weight ratio accounts for about 50-66% of debris flow) can form hyperconcentrated viscous debris flow (the solid volume concentration is up to 70-80%) which is in a solid state with "neutral suspension quality". All grain including gravel without sorting appears to move as a similar whole. According to Friedman's sorting standard of fluid particle separation (Shanbei Group of Chengdu Geological College, 1978), when  $\sigma_\phi > 2.6 \phi$ , the degree of sorting is the

worst. The degree of sorting of sandy flood ( $\sigma_\phi$  is  $0.99 \phi$ ) and diluent debris flow ( $\sigma_\phi$  is  $1.41 \phi$ ) are worse, while the degree of sorting of viscous debris flow ( $\sigma_\phi$  is  $4.28-4.5 \phi$ ) is very poor or no sorting at all. Its sorting is similar with those of the samples from its formation areas ( $\sigma_\phi = 4.4 \phi$ ) and deposition areas ( $\sigma_\phi = 4.05 \phi$ ). It is affected by the factors of short transportation distance and fast deposit speed of solid materials in viscous debris flow, but the most important factor is the overall movement of the fluid. Therefore, the sorting coefficient is often used as an indicator reflecting the moving process and deposit status of debris flow.

Cumulative probability curves of viscous debris flows can express different moving ways of solid particles in shearing flow ground. The cumulative probability curves of sandy flood and debris flow are double hops of concave and convex peak respectively because of the shearing difference between the fluid viscous force and the turbulent dispersive stress. The different forms of cumulative probability curves in Figure 7 show that the curve of sandy flood (curve 1) is the concave line, and the curve of diluent debris flow (curve 2) is the convex line. They are clearly divided into suspended moving section and push moving section, therefore, the sorting is good. While the

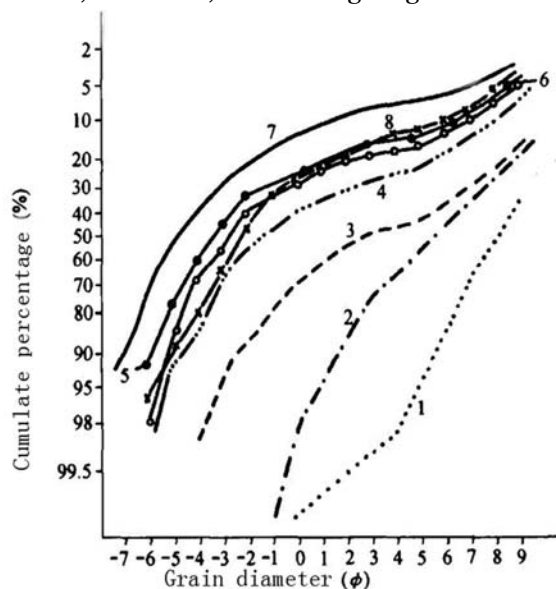


**Figure 7** Cumulative probability curves of viscous debris flows. 1.Sandy flood; 2. Diluent debris flow; 3. Transition debris flow; 4. Low concentrated viscous debris flow; 5. Medium concentrated viscous debris flow; 6. Hyperconcentrated viscous debris flow; 7. Sample from formation area; 8. Sample from deposition area.

curves of viscous debris flows (curves 4-6) are smooth convex curves, or called the double-jump upward angle convex curve. The distribution of particle size ranges widely. There are suspending segment and moving segment, but not very obvious, so the cumulative probability curve of viscous debris flow is called smooth curve of the overall movement. Therefore, there is very bad sorting or no sorting at all. The curve 4, 5, 6 in Figure 7 respectively represent the cumulative probability curve of low, medium and high concentrated viscous debris flow collected at Jiangjiagou Ravine, and their solid volumes are 0.6876, 0.7406 and 0.801 respectively. These findings further explain why hyperconcentrated viscous debris flow (with the volume concentration of solid up to 80%) can rapidly move on low-gradient ( $3-5^\circ$ ) ravines with velocity at  $10-18 \text{ m}\cdot\text{s}^{-1}$ . Figure 8 is a photo of the surge of debris flow taken on July 1, 2008. The picture shows that debris flow was in a very thick state like solid. The solid volume concentration of this debris flow is 0.7588, the velocity is  $7.8 \text{ m}\cdot\text{s}^{-1}$ , and the discharge is  $764.4 \text{ m}^3\cdot\text{s}^{-1}$ .



**Figure 8** Photo of the surge of high-concentrated viscous debris flow taken on July 1, 2008 at Jiangjiagou Ravine, Yunnan, China

We can conclude from the above analysis about the storage modulus and loss modulus of debris flow that hyperconcentrated debris flow is like cement concrete which is just made, and is like solid mass with viscous, elastic and plastic behaviors (Shijbannofe 1982). Therefore, it further reveals the rheological behaviors of slope loose mass from solid to liquid. Debris flow, as a hyperconcentrated solid water air mixture, has

become one of major natural disasters in mountain areas for its abrupt occurrence, great force and great destructive power. The experimental study on the viscoelastic stress-strain behaviors of debris flow slurry will contribute to a further study on the internal mechanism of the rheological properties of debris flow, and have great significance in developing practical forecasting system based on warning value of rainfall, designing the velocity parameters of debris flow controlling engineering effectively, protecting the safety of lives and property in mountain areas and the sustainable socio-economic development and so on.

#### 4 Conclusion and Discussion

(1) The rheological dynamic oscillatory tests about the debris flow slurry from Jiangjiagou Ravine reveals that the viscoelastic properties of slurry samples includes storage modulus and loss modulus, and they change with the changing of angular velocity (frequency).

(2) The analysis of rheological dynamic oscillatory tests about the debris flow slurry by using Gauss coordinate system shows that the rheological behaviors of debris flow slurry belong to the typical behaviors of viscoelastic fluid. In a separate study, storage modulus not only increases with the increasing of concentration of debris flow slurry, but also is affected by the content of coarse particles (sand). The higher the proportion of coarse particles is, the greater the storage modulus is. Therefore, this experiment further explains why hyperconcentrated viscous debris flow (with the volume concentration of solid up to 80%, coarse particles whose diameter is larger than 2mm account for about 50-66% of debris flow) can rapidly move on low-gradient ( $3-5^\circ$ ) ravines with velocity at  $10-18 \text{ m}\cdot\text{s}^{-1}$ .

(3) The analysis of  $G'$ ,  $G''$ ,  $G^*$  and  $\tan \delta$  by using the Theorem of Pythagoras shows the coexistence of the viscous response and the elastic response within the changing range of angular velocity, namely when the hyperconcentrated debris flow moves with a high speed overall, there are both solid-like behaviors and the behaviors of viscous fluid. Therefore, this experiment reveals the hyperconcentrated viscous debris flow is like cement concrete which is just made, and is like

solid mass with viscous, elastic and plastic behaviors.

(4) The analysis of  $\tan\delta$  further confirms that natural gravelly soil (solid) on steep slopes will suddenly become thixotropic liquefaction (liquid) under extreme heavy rainfall. Gel state is the critical point.

(5) The quantitative test and analysis about the viscoelastic behaviors of different viscous debris flows from triggering, thixotropy and shearing movement were not developed both at home and abroad for the restrictions of rheological

equipments. At present, there is only the quantitative test and analysis about the viscoelastic behaviors of debris flow slurry.

## Acknowledgments

This research is supported by the Youth Talent Team Program of Institute of Mountain Hazards and Environment, CAS and the National Natural Science Foundation of China (Grant No. 406710260).

## References

- Bagnold RA (1994). Experiments on a gravity-free dispersion of large solid spheres in a Newtonian fluid under shear. *Proceedings of the Royal Society of London A* 225: 49-63.
- Gebhard S (Li XH translated) (1998). A practical approach to rheology and rheometry. HAAKE. Oil Industry Publishing. pp 1-10, Beijing. (In Chinese)
- Haake Information Report V91-40E (1991). Elastic and its effect upon hold-filling. Karlsruhe, Germany. pp 10-12.
- Huang DN, Shen W (1983). Structure and rheological properties of newly-made concrete. China Architecture and Building Press. pp 2-12, Beijing. (In Chinese)
- Iverson RM (1989). Dynamic pore-pressure fluctuations in rapidly shearing granular materials. *Advancement of science* AA 246: 796-799.
- Jan CD, Shen HW (1997). Review dynamic modeling of debris flow. *Lecture Notes in Earth Sciences* 64: 93-116.
- Major JJ (1994). Experimental studies of deposition at a debris flow flume. USGS open in field report. pp 0-28.
- Pierson TC (1981). Dominant particle support mechanisms in debris flows at Mt. Thomas, New Zealand, and implications for flow mobility. *Journal of Sedimentation* 28: 49-60.
- Qian N (1989). Movement of hyper-concentration flow. Tsinghua University Publishing Company, Beijing. pp 27-40. (In Chinese)
- Schatzmann M, Fischer P, Bezzola GR (2003). Rheological behavior of fine and large particle suspensions. *Journal of Hydraulic Engineering* ASCE (10): 796-803.
- Shanbei Group of Chengdu Geological College (1978). Granularity analysis and appliance of sediment. Geological Publishing Company, Beijing. pp 553-565. (In Chinese)
- Shen SC, Wei H (1998). The constructive relation of debris flow. *Research on Mountain Disasters and Environmental Protection across Taiwan Strait* 1: 114-121. (In Chinese)
- Shijbannofe GC (Mong H translated) (1982). Basic characteristics and measure method of debris flows. Chongqing Branch of Science Technology Publishing Company, Chongqing. pp 100-103. (In Chinese)
- Thomas G, Mezger (2006). *The rheology hand for users of rotational and oscillatory rheometers*. 2nd revised edition. Stuttgart Coating Compendia 116-124.
- Vieyamofe CC (1987). *Rheological theory of solid mechanics*. Science Publishing Company, Beijing. pp 42-46. (In Chinese)
- Wang YY, Fei YJ (1999). Particle support mechanism in viscous debris flows at Jiangjia Ravine, China. *Science in China (series E)* 42 (5): 550-555.
- Wang YY, Fei XJ (2000). A modified rheological model of natural debris flows. *Chinese Science Bulletin* 45(8):743-747.
- Wang YY, Jan CD, Han WL, et al. (2004). Experimental research on the stress constitute relation of viscous debris flow. *Journal of Natural Disasters* 13(3): 33-38. (In Chinese)
- Wang YY, Tan RZ, Jan CD, et al. (2009). Study on the phenomena of gravels accumulated in deposits of viscous debris-flow with hyper-concentration. *Journal of Mountain Sciences* 2009(6): 88-95.
- Yao XL, Cheng YS (1986). *Physics of soil*. Agriculture Publishing Company, Beijing. pp 49-61. (In Chinese)
- Zhang ZY, Wang SF (1981). *Analyzed principle of engineering geology*. Geological Publishing Company, Beijing. pp 57-96. (In Chinese)